



**HAL**  
open science

# Bayesian Sparse Estimation of a Radar Scene with Weak and Strong Targets

Marie Lasserre, Stéphanie Bidon, Olivier Besson, François Le Chevalier

► **To cite this version:**

Marie Lasserre, Stéphanie Bidon, Olivier Besson, François Le Chevalier. Bayesian Sparse Estimation of a Radar Scene with Weak and Strong Targets. 2015 3rd International Workshop on Compressed Sensing Theory and its Applications to Radar, Sonar, and Remote Sensing (CoSeRa), Jun 2015, Pisa, Italy. pp. 51-55. hal-01446139

**HAL Id: hal-01446139**

**<https://hal.science/hal-01446139>**

Submitted on 25 Jan 2017

**HAL** is a multi-disciplinary open access archive for the deposit and dissemination of scientific research documents, whether they are published or not. The documents may come from teaching and research institutions in France or abroad, or from public or private research centers.

L'archive ouverte pluridisciplinaire **HAL**, est destinée au dépôt et à la diffusion de documents scientifiques de niveau recherche, publiés ou non, émanant des établissements d'enseignement et de recherche français ou étrangers, des laboratoires publics ou privés.



## Open Archive TOULOUSE Archive Ouverte (OATAO)

OATAO is an open access repository that collects the work of Toulouse researchers and makes it freely available over the web where possible.

This is an author-deposited version published in: <http://oatao.univ-toulouse.fr/>  
Eprints ID: 16750

**To cite this version:** Lasserre, Marie and Bidon, Stéphanie and Besson, Olivier and Le Chevalier, François *Bayesian Sparse Estimation of a Radar Scene with Weak and Strong Targets*. (2015) In: 2015 3rd International Workshop on Compressed Sensing Theory and its Applications to Radar, Sonar, and Remote Sensing (CoSeRa), 16 June 2015 - 19 June 2015 (Pisa, Italy).

Official URL: <http://dx.doi.org/10.1109/CoSeRa.2015.7330262>

Any correspondence concerning this service should be sent to the repository administrator: [staff-oatao@listes-diff.inp-toulouse.fr](mailto:staff-oatao@listes-diff.inp-toulouse.fr)

# Bayesian Sparse Estimation of a Radar Scene with Weak and Strong Targets

Marie Lasserre, Stéphanie Bidon and Olivier Besson  
 DEOS/ISAE,  
 University of Toulouse, Toulouse, France  
 Email: firstname.lastname@isae.fr

François Le Chevalier  
 MS<sup>3</sup>  
 Delft University of Technology, Delft, The Netherlands  
 Email: F.LeChevalier@tudelft.nl

**Abstract**—We consider the problem of estimating a finite number of atoms of a dictionary embedded in white noise, using a sparse signal representation (SSR) approach, a problem which is relevant in many radar applications. In particular, the estimation of a radar scene consisting of targets with wide amplitude range can be challenging since the sidelobes of a strong target can disrupt the estimation of a weak one. In this paper, we present a Bayesian algorithm able to estimate weak targets possibly hidden by strong ones. The main strength of this algorithm lies in a novel sparse-promoting prior distribution which decorrelates sparsity level and target power and makes the estimation process span the whole target power range. This algorithm is implemented through a Monte-Carlo Markov chain. It is successfully evaluated on synthetic and semiexperimental radar data.

## I. INTRODUCTION

A well-known problem in radar applications is the estimation of radar scenes containing strong and weak targets, since the sidelobes of a strong target can disrupt the estimation of a weak one. Several algorithms were developed to address this issue, starting with the CLEAN algorithm [1], [2]. This algorithm “successively removes large targets and their sidelobe responses by subtracting the point spread function of the receiving system centered at the locations of the bright targets” [2]. Thus, if a strong target and a weak target are present in the radar scene, the strong target will first be removed, and then the weak target should appear as the bright target and be estimated. More recently, the so-called “greedy methods”, such as the Matching Pursuit (MP) [3] and Orthogonal Matching Pursuit (OMP) [4], [5], use a similar procedure to estimate such a target scene. Generally speaking, the estimation methods that rely on a sparse representation of the target scene are of particular interest in this issue since they allow the estimation of a sidelobe-less signal of interest (SOI) and can lead to a better target dynamic range.

In [6], a Bayesian sparse recovery algorithm was developed and proved to give good performance on synthetic and experimental data. As in every sparse signal representation (SSR) approach, the signal is described as a linear combination of a finite number of atoms from a dictionary. Using this approach, the problem can be written as

$$\mathbf{y} = \mathbf{F}\mathbf{x} + \mathbf{n} \quad (1)$$

The work of M. Lasserre, S. Bidon and O. Besson is supported by the Délégation Générale de l’Armement under grant 2012.60.0012.00.470.75.01.

with

$\mathbf{F} \in \mathbb{C}^{M \times \bar{M}}$  a sparsifying dictionary of size  $M \times \bar{M}$  where usually  $\bar{M} \geq M$  ;  
 $\mathbf{x} \in \mathbb{C}^{\bar{M}}$  the sparse vector having ideally exactly  $N$  nonzero components,  $N$  being the number of scatterers in the target scene.

However, as in every SSR algorithm, adequate tuning of some parameters is essential since it can deteriorate the performance of the reconstruction. In [6], the sparsity is enforced via a sparse-promoting prior distribution on vector  $\mathbf{x}$ . This prior depends on some hyperparameters that will adjust the knowledge the radar operator has about the target power level. In this case, setting up these hyperparameters can be tedious. This paper aims at modifying the algorithm proposed in [6] in order to deal with targets having significant different power level. The approach proposed is to modify the prior distribution of the sparse vector and to divide its support into several classes, which correspond to subdivisions of the receiver dynamic range. Thus, the estimation process is “forced” to span each class of target power.

The remaining of the paper is organized as follows. The proposed Bayesian model is described in Section II, as well as the associated estimation scheme in Section III. The proposed algorithm is successfully evaluated via numerical simulations on both synthetic and semiexperimental data in Section IV.

## II. BAYESIAN MODEL

In this section, we describe the hierarchical Bayesian model adopted, which is represented graphically in Fig. 1. A Bayesian framework is established in order to estimate the target scene  $\mathbf{x}$ . Thus, each unknown parameter is modeled by a random variable with a given prior probability density function (pdf). Each prior density is chosen as facilitating the computation of the estimation process (mathematical tractability), yet preserving physical sense to the hierarchical model.

### A. Likelihood

We adopt the same observation model as in [6] recalled in (1). An additive white noise background is considered, and the noise  $\mathbf{n}$  is assumed to be centered Gaussian with power  $\sigma^2$ , which is denoted as

$$\mathbf{n} | \sigma^2 \sim \mathcal{CN}_M(\mathbf{0}, \sigma^2 \mathbf{I}) \quad (2)$$

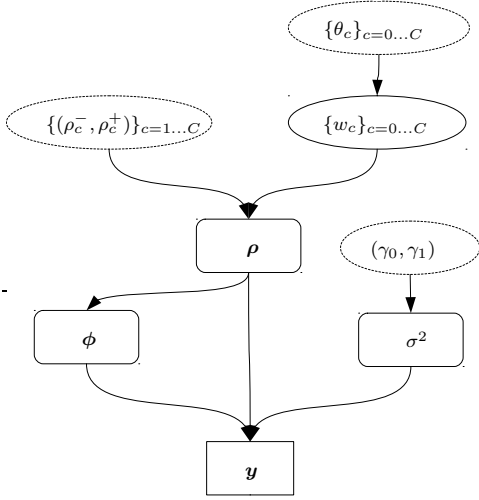


Fig. 1. Directed acyclic graph associated with the hierarchical Bayesian model proposed. The parameters in the dashed circles need to be adjusted by the operator.

where  $\mathbf{I}$  is the identity matrix. The likelihood function is thus given by

$$f(\mathbf{y}|\mathbf{x}, \sigma^2) = \frac{1}{\pi^M \sigma^{2M}} \exp \left\{ -\frac{\|\mathbf{y} - \mathbf{F}\mathbf{x}\|_2^2}{\sigma^2} \right\}. \quad (3)$$

### B. Prior pdfs of the parameters

1) *Noise power  $\sigma^2$* : As in [6], an inverse-gamma prior is chosen for the white noise power  $\sigma^2$ , essentially because it is conjugate to the likelihood (3). The prior pdf of  $\sigma^2$  can therefore be expressed as

$$\pi(\sigma^2|\gamma_0, \gamma_1) \propto \frac{e^{-\gamma_1/\sigma^2}}{(\sigma^2)^{\gamma_0+1}} \mathbb{I}_{[0,+\infty)}(\sigma^2) \quad (4)$$

where  $\gamma_0, \gamma_1$  are respectively the shape and scale parameters. The distribution (4) is denoted as  $\sigma^2|\gamma_0, \gamma_1 \sim \mathcal{IG}(\gamma_0, \gamma_1)$ . As mentioned before, the shape and scale parameters  $(\gamma_0, \gamma_1)$  allow a very informative, or on the contrary flat, prior distribution to be selected.

2) *Sparse vector  $\mathbf{x}$* : As said in Section I, the approach chosen to deal with the problem of estimating targets with different power level is to consider several classes of target power. Truncating the power range makes sense in radar applications since the receiver has some predefined dynamic range [7, chap.11]. Then, the idea is to divide the power range into several classes, within the dynamic range limitation.

The elements  $x_{\bar{m}} \triangleq [\mathbf{x}]_{\bar{m}}$  of the amplitude vector are assumed independent and identically distributed (iid). Instead of considering  $\mathbf{x} \in \mathbb{C}^M$ , we parametrize  $\mathbf{x}$  in terms of modulus  $\rho$  and angle  $\phi$  subject to (s.t.)

$$\mathbf{x} \triangleq \boldsymbol{\rho} \odot e^{i\boldsymbol{\phi}}, \quad (5)$$

where  $\odot$  refers to the Hadamard product. Eq. (5) is equivalent to the formulation  $\forall \bar{m} \in \{0 \dots M-1\}, x_{\bar{m}} = \rho_{\bar{m}} e^{i\phi_{\bar{m}}}$ .

The elements in  $\boldsymbol{\rho}$  and  $\boldsymbol{\phi}$  are iid *a priori*. The Bernoulli-Gaussian prior distribution on  $x_{\bar{m}}$  used in [6] can be modified in order to include this idea of classes of target power, such that

$$\pi(\rho_{\bar{m}}|\mathbf{w}) = w_0 \delta(\rho_{\bar{m}}) + \sum_{c=1}^C \frac{w_c k_c}{\sqrt{2\pi\sigma_c^2}} \exp \left\{ -\frac{1}{2\sigma_c^2} (\rho_{\bar{m}} - \rho_c)^2 \right\} \mathbb{I}_{[\rho_c^-, \rho_c^+]}(\rho_{\bar{m}}) \quad (6)$$

and

$$\pi(\phi_{\bar{m}}|\rho_{\bar{m}} = 0) = \delta(\phi_{\bar{m}}) \quad (7a)$$

$$\pi(\phi_{\bar{m}}|\rho_{\bar{m}} \neq 0) = \frac{1}{2\pi} \mathbb{I}_{[0, 2\pi]}(\phi_{\bar{m}}) \quad (7b)$$

where  $\mathbf{w} = [w_c]_{c=0, \dots, C}$  is the vector of class probabilities, and  $w_0 = 1 - \sum_{c=1}^C w_c$ .  $k_c$  is a scaling constant consecutive to the truncation of the Gaussian on  $[\rho_c^-, \rho_c^+]$ . This mixed-type prior distribution allows to enforce sparsity while including the target power classes notion. In other words,  $\rho_{\bar{m}}$  belongs to class  $c$  with probability  $w_c$ , and is distributed following  $\mathcal{N}_{[\rho_c^-, \rho_c^+]}(\rho_c, \sigma_c^2)$ ; it is null with probability  $w_0$ .  $\rho_c$  and  $\sigma_c^2$  represent the mean and variance in each class. Thus, the hyperparameters  $\{(\rho_c^-, \rho_c^+, \rho_c, \sigma_c^2)\}_{c=1 \dots C}$  can be set-up such that the distributions  $\mathcal{N}_{[\rho_c^-, \rho_c^+]}(\rho_c, \sigma_c^2)$  cover the whole expected amplitude range, while having separated or almost-separated supports.

However, setting-up the parameters  $\{(\rho_c, \sigma_c^2)\}_{c=1 \dots C}$  can be tedious, so a simpler prior can be assigned to  $\rho_{\bar{m}}$ , e.g., a uniform-like prior

$$\pi(\rho_{\bar{m}}|\mathbf{w}) = w_0 \delta(\rho_{\bar{m}}) + \sum_{c=1}^C w_c k_c \mathbb{I}_{[\rho_c^-, \rho_c^+]}(\rho_{\bar{m}}). \quad (8)$$

In this case,  $\rho_{\bar{m}}$  belongs to class  $c$  with probability  $w_c$ , and is uniformly distributed within this class; it is null with probability  $w_0$ . In the following, we adopt this simpler uniform-like prior distribution, acknowledging that it is still possible to adopt a Gaussian-like prior distribution (6).

### C. Prior pdfs of the hyperparameters

1) *Vector of class probabilities  $\mathbf{w}$* : A conventional solution for the distribution of the vector of class probabilities  $\mathbf{w}$  is a multivariate Dirichlet distribution with concentration parameters  $\theta_0, \dots, \theta_C > 0$  [8], denoted as  $\mathbf{w} \sim \text{Dir}(\theta_0, \dots, \theta_C)$

$$\pi(\mathbf{w}|\theta_0, \dots, \theta_C) \propto w_0^{\theta_0-1} \mathbb{I}_{[0,1]}(w_0) \times \prod_{c=1}^C w_c^{\theta_c-1} \mathbb{I}_{[0,1]}(w_c). \quad (9)$$

When no prior information about the target power range is available, a symmetric Dirichlet distribution can be adopted where the concentration parameters  $\theta_0, \dots, \theta_C$  are equals to 1. Otherwise, the concentration parameters can be adjusted in order to favor some classes over the other ones.

### III. BAYESIAN ESTIMATION

Herein we propose an estimation scheme of the target scene  $\mathbf{x}$  based on the Bayesian hierarchical model described in (3), (7), (8), (9). More precisely, our objective is to obtain the following estimator of  $\mathbf{x}$

$$\hat{\mathbf{x}}_{\text{class}} = \mathcal{E} \{ \boldsymbol{\rho} \odot e^{i\phi} | \mathbf{y} \} \quad (10)$$

$$= \int_{\boldsymbol{\rho}, \phi} \boldsymbol{\rho} \odot e^{i\phi} f(\boldsymbol{\rho}, \phi | \mathbf{y}) d\boldsymbol{\rho} d\phi. \quad (11)$$

This last integral is intractable to derive analytically, so we demarginalize it and calculate  $\hat{\mathbf{x}}_{\text{class}}$  as

$$\hat{\mathbf{x}}_{\text{class}} = \int_{\sigma^2, \boldsymbol{\rho}, \phi, \mathbf{w}} \boldsymbol{\rho} \odot e^{i\phi} f(\sigma^2, \boldsymbol{\rho}, \phi, \mathbf{w} | \mathbf{y}) d\sigma^2 d\boldsymbol{\rho} d\phi d\mathbf{w}. \quad (12)$$

It is now possible to compute  $\hat{\mathbf{x}}_{\text{class}}$  since we can obtain samples following the joint posterior distribution  $f(\sigma^2, \boldsymbol{\rho}, \phi, \mathbf{w} | \mathbf{y})$ . Indeed, as in [6], a Monte-Carlo Markov Chain (MCMC) is implemented [9]. More specifically, a Gibbs sampler [9, chap.10] is used, which simulates iteratively samples  $\sigma^{2(t)}$ ,  $\boldsymbol{\rho}^{(t)}$ ,  $\phi^{(t)}$ ,  $\mathbf{w}^{(t)}$  according to their conditional posterior distribution  $f(\zeta_i | \mathbf{y}, \zeta_{-i})$ , where  $\zeta = [\sigma^2, \boldsymbol{\rho}^T, \phi^T, \mathbf{w}^T]^T$  and  $\zeta_{-i}$  is the vector  $\zeta$  whose  $i$ th element has been removed. After a burn-in time  $N_{bi}$ , the samples  $\zeta^{(t)}$  are distributed according to the joint posterior distribution  $f(\zeta | \mathbf{y})$ . When enough samples are acquired (namely,  $N_r$ ), the estimator of  $\mathbf{x}$  is built empirically as

$$\hat{\mathbf{x}}_{\text{class}} = N_r^{-1} \sum_{t=1}^{N_r} \boldsymbol{\rho}^{(t+N_{bi})} \odot e^{i\phi^{(t+N_{bi})}} \quad (13)$$

which is the empirical mean of all the samples  $\mathbf{x}^{(t)} = \boldsymbol{\rho}^{(t)} \odot e^{i\phi^{(t)}}$ . The conditional posterior distributions are obtained from the joint posterior pdf of  $\boldsymbol{\rho}, \phi, \sigma^2, \mathbf{w} | \mathbf{y}$

$$f(\boldsymbol{\rho}, \phi, \sigma^2, \mathbf{w} | \mathbf{y}) \propto f(\mathbf{y} | \boldsymbol{\rho}, \phi, \sigma^2) \pi(\boldsymbol{\rho} | \mathbf{w}) \pi(\phi | \boldsymbol{\rho}) \pi(\sigma^2) \pi(\mathbf{w}). \quad (14)$$

#### A. Sampling of $\boldsymbol{\rho}$

Since the elements in  $\boldsymbol{\rho}$  are *a priori* iid, it is sampled element-wise. Thus, we calculate the conditional posterior distribution of  $\rho_{\bar{m}}$  using (8) and (14)

$$\begin{aligned} f(\rho_{\bar{m}} | \mathbf{y}, \sigma^2, \boldsymbol{\rho}_{-\bar{m}}, \phi, \mathbf{w}) &\propto f(\mathbf{y} | \boldsymbol{\rho}, \phi, \sigma^2) \pi(\boldsymbol{\rho} | \mathbf{w}) \\ &\propto \exp \left\{ -\sigma^{-2} \left[ \rho_{\bar{m}}^2 \|\mathbf{f}_{\bar{m}}\|^2 - 2\rho_{\bar{m}} \operatorname{Re} \{ \mathbf{e}_{\bar{m}}^H \mathbf{f}_{\bar{m}} e^{i\phi_{\bar{m}}} \} \right] \right\} \\ &\times \left[ w_0 \delta(\rho_{\bar{m}}) + \sum_{c=1}^C w_c k_{\bar{m},c} \mathbb{I}_{[\rho_c^-, \rho_c^+]}(\rho_{\bar{m}}) \right] \\ &\propto w_{\bar{m},0} \delta(\rho_{\bar{m}}) \\ &+ \sum_{c=1}^C \frac{w_{\bar{m},c} k_{\bar{m},c}}{\sqrt{2\pi\eta_{\bar{m}}^2}} \exp \left\{ -\frac{1}{2\eta_{\bar{m}}^2} (\rho_{\bar{m}} - \mu_{\bar{m}})^2 \right\} \mathbb{I}_{[\rho_c^-, \rho_c^+]}(\rho_{\bar{m}}) \end{aligned} \quad (15)$$

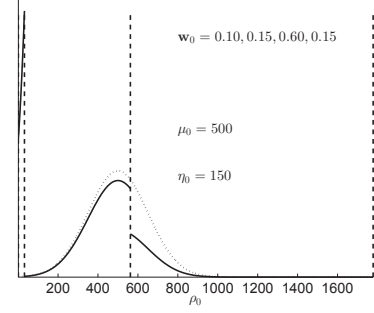


Fig. 2. Conditional posterior distribution (15) of  $\rho_0$  with  $\mu_0 = 500$ ,  $\eta_0 = 150$  and  $\mathbf{w}_0 = [0.10, 0.15, 0.60, 0.15]$ . The dashed lines represent the limits of the three non-zero power classes. The dotted curve is the Gaussian  $\mathcal{N}(\mu_{\bar{m}}, \eta_{\bar{m}}^2)$ .

where for  $c = 1, \dots, C$

$$\eta_{\bar{m}}^2 = \frac{1}{2} \sigma^2 \|\mathbf{f}_{\bar{m}}\|^{-2} \quad (15a)$$

$$\mu_{\bar{m}} = \|\mathbf{f}_{\bar{m}}\|^{-2} \operatorname{Re} \{ \mathbf{e}_{\bar{m}}^H \mathbf{f}_{\bar{m}} e^{i\phi_{\bar{m}}} \} \quad (15b)$$

$$w_{\bar{m},c} = \frac{w_c \times \frac{k_{\bar{m},c}}{k_{\bar{m},c}} (2\pi\eta_{\bar{m}}^2)^{1/2} \exp \left\{ \frac{1}{2} \eta_{\bar{m}}^{-2} \mu_{\bar{m}}^2 \right\}}{w_0 + \sum_{c=1}^C w_c \frac{k_{\bar{m},c}}{k_{\bar{m},c}} (2\pi\eta_{\bar{m}}^2)^{1/2} \exp \left\{ \frac{1}{2} \eta_{\bar{m}}^{-2} \mu_{\bar{m}}^2 \right\}} \quad (15c)$$

and  $w_{\bar{m},0} = 1 - \sum_{c=1}^C w_{\bar{m},c}$ . The conditional posterior distribution of  $\rho_{\bar{m}}$  is then a mixed-type distribution with an atom at 0 and a continuous component which is a mixture of truncated Gaussians that are easy to simulate from, using for instance an accept-reject procedure [10]. Note that the mean and variance of the truncated Gaussian  $\mathcal{N}_{[\rho_c^-, \rho_c^+]}(\mu_{\bar{m}}, \eta_{\bar{m}}^2)$  do not depend on the class, but that this Gaussian is weighted by  $w_{\bar{m},c}$ , which may be different for each class. This is illustrated in Fig.2 where we can see an example of this distribution, without the discrete component.

**Remark.** When using a Fourier dictionary,  $\|\mathbf{f}_{\bar{m}}\|^2 = 1$  so that  $\eta_{\bar{m}}^2 = \sigma^2/2$ , which does not depend on the grid index  $\bar{m}$ .

#### B. Sampling of $\phi$

The elements in  $\phi$  are also *a priori* iid so it is sampled element-wise. The conditional posterior distribution of  $\phi_{\bar{m}}$  is written as

$$\begin{aligned} f(\phi_{\bar{m}} | \mathbf{y}, \sigma^2, \boldsymbol{\rho}_{-\bar{m}}, \boldsymbol{\rho}) &\propto f(\mathbf{y} | \boldsymbol{\rho}, \phi, \sigma^2) \pi(\phi_{\bar{m}} | \rho_{\bar{m}}) \\ &\propto \exp \left\{ -\sigma^{-2} \left[ -2\rho_{\bar{m}} \operatorname{Re} \{ \mathbf{e}_{\bar{m}}^H \mathbf{f}_{\bar{m}} e^{i\phi_{\bar{m}}} \} \right] \right\} \pi(\phi_{\bar{m}} | \rho_{\bar{m}}) \\ &\propto \exp \left\{ 2\sigma^{-2} \rho_{\bar{m}} |\mathbf{f}_{\bar{m}}^H \mathbf{e}_{\bar{m}}| \cos(\phi_{\bar{m}} - \psi_{\bar{m}}) \right\} \pi(\phi_{\bar{m}} | \rho_{\bar{m}}). \end{aligned}$$

According to (7a), we have

$$f(\phi_{\bar{m}} | \mathbf{y}, \sigma^2, \boldsymbol{\rho}_{-\bar{m}}, \boldsymbol{\rho}; \rho_{\bar{m}} = 0) = \delta(\phi_{\bar{m}}) \quad (16)$$

and

$$\begin{aligned} f(\phi_{\bar{m}} | \mathbf{y}, \sigma^2, \boldsymbol{\rho}_{-\bar{m}}, \boldsymbol{\rho}; \rho_{\bar{m}} \neq 0) &\propto \\ &\exp \{ \kappa_{\bar{m}} \cos(\phi_{\bar{m}} - \psi_{\bar{m}}) \} \mathbb{I}_{[0, 2\pi]}(\phi_{\bar{m}}) \end{aligned} \quad (17)$$

which is a von Mises-Fisher distribution with concentration parameter and mean direction respectively [11]

$$\kappa_{\bar{m}} = 2\rho_{\bar{m}}\sigma^{-2}|\mathbf{f}_{\bar{m}}^H \mathbf{e}_{\bar{m}}| \quad (17a)$$

$$\psi_{\bar{m}} = \angle \mathbf{f}_{\bar{m}}^H \mathbf{e}_{\bar{m}} \quad (17b)$$

where  $\angle$  represents the angle in  $[0, 2\pi)$ . It is denoted as  $\phi_{\bar{m}}|\mathbf{y}, \sigma^2, \phi_{-\bar{m}}, \boldsymbol{\rho}; \rho_{\bar{m}} \neq 0 \sim \mathcal{VM}(\kappa_{\bar{m}}, \psi_{\bar{m}})$ . This distribution is easy to simulate from following the method described in [11].

### C. Sampling of $\sigma^2$

As in [6], the conditional posterior distribution of  $\sigma^2$  is

$$\sigma^2|\mathbf{y}, \boldsymbol{\rho}, \phi \sim \mathcal{IG}(\gamma_0 + M, \gamma_1 + \|\mathbf{y} - \mathbf{F}(\boldsymbol{\rho} \odot e^{i\phi})\|_2^2). \quad (18)$$

### D. Sampling of $\mathbf{w}$

A Dirichlet prior distribution is assigned to vector  $\mathbf{w}$ . Using (9) and (14), the conditional posterior distribution of  $\mathbf{w}$  is then calculated as

$$\begin{aligned} f(\mathbf{w}|\mathbf{y}, \boldsymbol{\rho}) &\propto \pi(\boldsymbol{\rho}|\mathbf{w})\pi(\mathbf{w}) \\ &\propto \prod_{\bar{m}=0}^{\bar{M}-1} \left\{ w_0 \delta(\rho_{\bar{m}}) + \sum_{c=1}^C w_c k_c \mathbb{I}_{[\rho_c^-, \rho_c^+]}(\rho_{\bar{m}}) \right\} \\ &\quad \times w_0^{\theta_0-1} \prod_{c=1}^C w_c^{\theta_c-1} \\ &\propto w_0^{n_0+\theta_0-1} \times \prod_{c=1}^C w_c^{n_c+\theta_c-1} \end{aligned} \quad (19)$$

where  $n_c = \#\{\bar{m}|\rho_{\bar{m}} \in [\rho_c^-, \rho_c^+]\}$ , i.e., the number of scatterers in class  $c$ , and  $n_0 = \bar{M} - \sum_{c=1}^C n_c$ . Thus, the conditional posterior distribution of  $\mathbf{w}$  is a Dirichlet distribution with concentration parameters  $(n_0 + \theta_0, n_1 + \theta_1, \dots, n_C + \theta_C)$ .

## IV. NUMERICAL SIMULATIONS

### A. Synthetic data

First, the proposed algorithm is compared to the previous algorithm from [6] through numerical simulations on synthetic data. These are generated according to (1) and (2), and using a Fourier basis  $\mathbf{F}$  as a sparsifying dictionary. The target power classes adopted are:  $(-\infty, 0]$ ,  $[0, 30]$ ,  $[30, 55]$ ,  $[55, 65]$  dB. As mentioned before, when using the previous algorithm from [6], the radar operator must set-up the scale and shape parameters of the prior distribution of the target power via hyperparameters (see discussion in [6, Sec.III]). In what follows, they are adjusted to a non-informative Jeffreys prior, or to an informative prior corresponding to high or low-power targets. In this scenario, we consider a strong target with post-processing SNR of 60 dB, defined as ( $\mathbf{F}$  being unitary)

$$\text{SNR} = |x_{\bar{m}}|^2/\sigma^2, \quad (20)$$

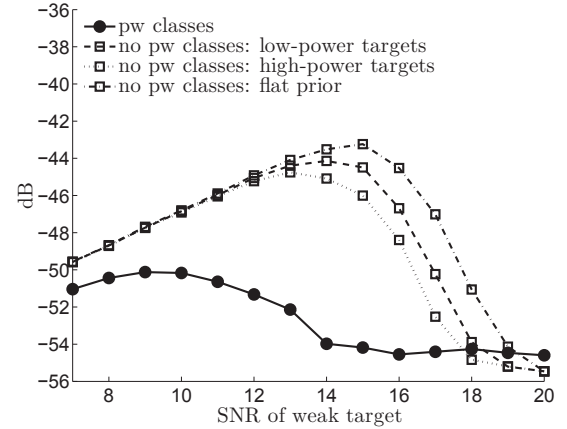
surrounded by two weak targets with varying SNR from 7 to 20 dB, located on the previous and next frequency bins. The three targets have random phase. The performance of these

two algorithms is assessed after  $N_{mc} = 200$  Monte-Carlo simulations through the calculation of the normalized Mean Square Error (nMSE) of the estimated target scene  $\mathbf{F}\hat{\mathbf{x}}_{\text{class}}$  and the nMSE of the elements of  $\hat{\mathbf{x}}_{\text{class}}$  corresponding to the position of the targets in the scene. They are respectively calculated as

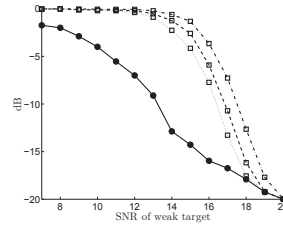
$$\text{nMSE}(\mathbf{F}\hat{\mathbf{x}}_{\text{class}}) = \frac{1}{N_{mc}} \sum_{n=1}^{N_{mc}} \frac{\|\mathbf{F}\hat{\mathbf{x}}_{\text{class}}^{(n)} - \mathbf{F}\mathbf{x}\|_2^2}{\|\mathbf{F}\mathbf{x}\|_2^2} \quad (21)$$

$$\text{nMSE}(\hat{x}_{\text{class}_i}) = \frac{1}{N_{mc}} \sum_{n=1}^{N_{mc}} \frac{|\hat{x}_{\text{class}_i}^{(n)} - x_i|^2}{|x_i|^2}. \quad (22)$$

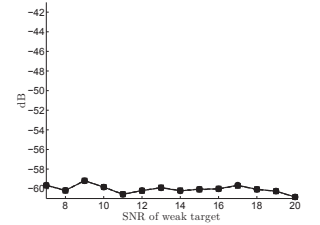
Fig.3 shows that the proposed algorithm with target power classes outperforms the algorithm from [6] in terms of nMSE of  $\mathbf{F}\mathbf{x}$ , regardless of the hyperparameters set-up. In fact, both algorithms give the same performance in terms of nMSE of the strong target ( $x_1$ , Fig.3(c)) but the proposed algorithm better estimates the weak targets (e.g.,  $x_0$ , Fig.3(b)).



(a) nMSE of  $\mathbf{F}\mathbf{x}$



(b) nMSE of  $x_0$



(c) nMSE of  $x_1$

Fig. 3. Comparison between the performance of the proposed algorithm with power classes (plain line), and that of the previous algorithm from [6] in the case of a flat prior (dash-dotted line), or a prior adjusted to high-power (dotted line) or low-power targets (dashed line). The scenario consists of three close targets separated by  $1/M$ .  $\bar{M} = M = 16$ .  $N_r = 1000$ ,  $N_{bi} = 200$ .

### B. Semiexperimental data

The performance of the proposed algorithm is finally confirmed on semiexperimental data recorded in November 2014 using the PARSAX radar [12] installed at TU Delft, The Netherlands. The semiexperimental data were built adding synthetic one-dimensional targets to a deramped thermal noise signal. The target scene is represented in Fig.4(a); it consists of

3 strong targets with SNR=60dB, a target at 35 dB and 3 weak targets near two of the strong ones. This target scene was processed range-bin-wise since the algorithm is limited to one-dimensional analysis for the moment. The proposed algorithm well estimates the target scene, especially the weak targets that are not always estimated by the previous algorithm from [6]. It is also interesting to see that the proposed algorithm estimates zero-velocity components that most probably correspond to offsets of the coders.

## V. CONCLUSION

In this paper we have presented a new Bayesian algorithm for the sparse representation of a radar scene with targets having wide amplitude range. In particular, a new sparse-promoting prior was introduced, whose aim is to consider several classes of target power and make the estimation process span each class. The algorithm proposed, though computationally intensive, allows to estimate weak targets whose recovery might have been disrupted by strong ones. The study was limited to on-grid targets but the algorithm will be extended in the near future in order to deal with off-grid targets.

## ACKNOWLEDGEMENT

The authors would like to thank O. Krasnov at TU Delft for kindly providing the PARSAX experimental data.

## REFERENCES

- [1] J. Hogbom, "Aperture Synthesis with a non-regular Distribution of Interferometer Baselines," *Astronomy and Astrophysics Supplement*, vol. 15, pp. 417–426, 1974.
- [2] J. Tsao and B. D. Steinberg, "Reduction of Sidelobe and Speckle Artifacts in Microwave Imaging: the Clean Technique." *IEEE Transactions on Antennas and Propagation*, vol. 36, no. 4, pp. 543–557, 1988.
- [3] S. G. Mallat and Z. Zhang, "Matching Pursuits With Time-Frequency Dictionaries," *IEEE transactions on signal processing*, vol. 41, no. 12, pp. 3397–3415, 1993.
- [4] Y. Pati, R. Rezaifar, and P. Krishnaprasad, "Orthogonal matching pursuit: recursive function approximation with applications to wavelet decomposition," *Proceedings of 27th Asilomar Conference on Signals, Systems and Computers*, pp. 40–44, 1993.
- [5] G. Davis, "Adaptive Greedy Approximations," *Constructive Approximation*, vol. 13, pp. 57–98, 1997.
- [6] S. Bidon, J.-Y. Tourneret, L. Savy, and F. Le Chevalier, "Bayesian sparse estimation of migrating targets for wideband radar," *IEEE Trans. Aerosp. Electron. Syst.*, vol. 50, no. 2, pp. 871–886, Apr. 2014.
- [7] M. A. Richards, J. A. Scheer, and W. A. Holm, Eds., *Principles of Modern Radar: Basic Principles*. Raleigh, NC: SciTech Publishing, 2010.
- [8] S. Kotz, N. Balakrishnan, and N. L. Johnson, *Continuous Multivariate Distributions*, 2nd ed. Wiley Series in Probability and Statistics, 2000, vol. 1.
- [9] C. Robert and G. Casella, *Monte Carlo Statistical Methods*. Springer, 2004.
- [10] C. P. Robert, "Simulation of truncated normal variables," *Statistics and Computing*, vol. 5, pp. 121–125, 1995.
- [11] D. J. Best and N. I. Fisher, "Efficient Simulation of the von Mises Distribution," *Journal of the Royal Statistical Society*, vol. 28, no. 2, pp. 152–157, 1979.
- [12] O. A. Krasnov, G. P. Babur, Z. Wang, L. P. Ligthart, and F. van der Zwan, "Basics and first experiments demonstrating isolation improvements in the agile polarimetric FM-CW radar – PARSAX," *International Journal of Microwave and Wireless Technologies*, vol. 2, pp. 419–428, 8 2010.

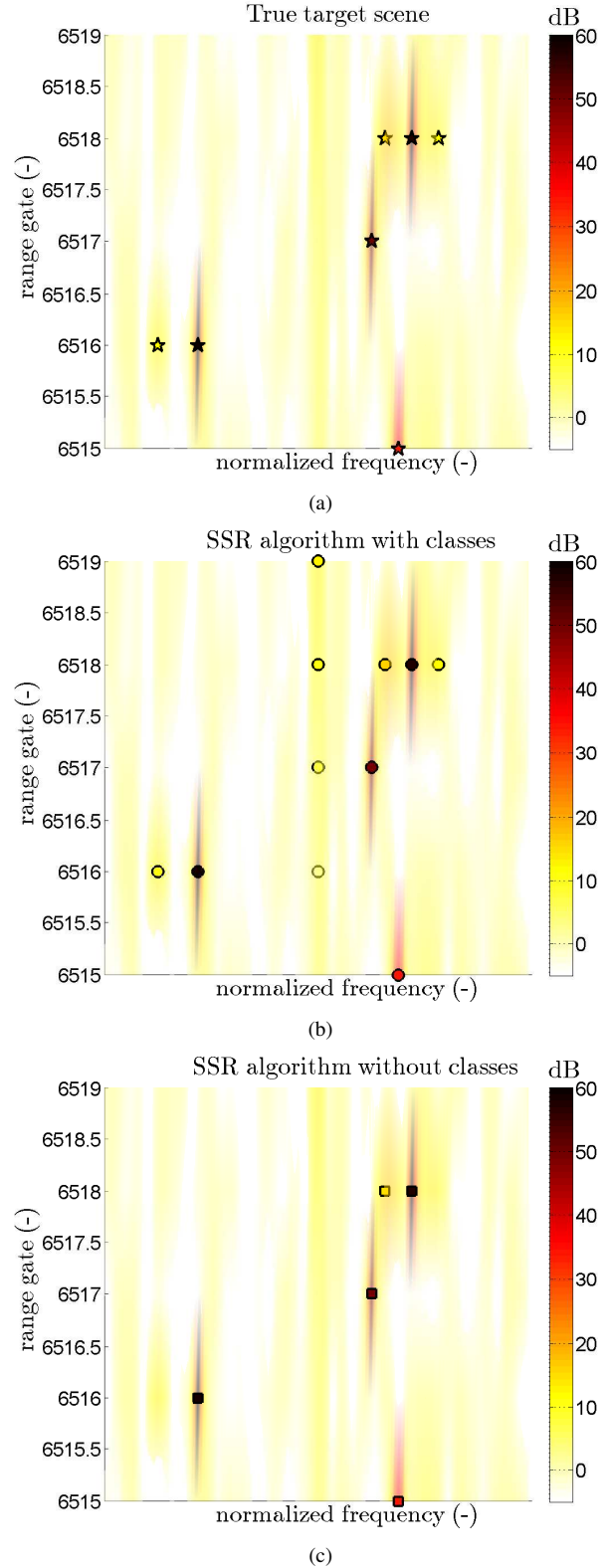


Fig. 4. Evaluation on semiexperimental data: 4(a) true target scene (stars) 4(b) target scene estimated by the proposed algorithm (circles) 4(c) target scene estimated by the previous algorithm from [6] (squares). The background corresponds to the target scene estimated by the APES algorithm.  $M = 32$ ,  $\bar{M} = M$ ,  $N_r = 1000$ ,  $N_{b_i} = 1000$ .